

Ab initio path integral Monte Carlo simulations of the uniform electron gas on large length scales

Tobias Dornheim,^{*,†} Sebastian Schwalbe,[†] Zhandos A. Moldabekov,[†] Jan
Vorberger,[‡] and Panagiotis Tolias[¶]

[†]*Center for Advanced Systems Understanding (CASUS), Helmholtz-Zentrum
Dresden-Rossendorf (HZDR), D-02826 Görlitz, Germany*

[‡]*Institute of Radiation Physics, Helmholtz-Zentrum Dresden-Rossendorf (HZDR), D-01328
Dresden, Germany*

[¶]*Space and Plasma Physics, Royal Institute of Technology (KTH), Stockholm, SE-100 44,
Sweden*

E-mail: t.dornheim@hzdr.de

Abstract

The accurate description of non-ideal quantum many-body systems is of prime importance for a host of applications within physics, quantum chemistry, material science, and related disciplines. At finite temperatures, the gold standard is given by *ab initio* path integral Monte Carlo (PIMC) simulations, which do not require any empirical input, but exhibit an exponential increase in the required compute time for fermionic systems with increasing the system size N . Very recently, it has been suggested to compute fermionic properties without this bottleneck based on PIMC simulations of fictitious identical particles. In the present work, we use this technique to carry out very large

($N \leq 1000$) PIMC simulations of the warm dense electron gas and demonstrate that it is capable of providing a highly accurate description of investigated properties, i.e., the static structure factor, the static density response function, and local field correction, over the entire range of length scales.

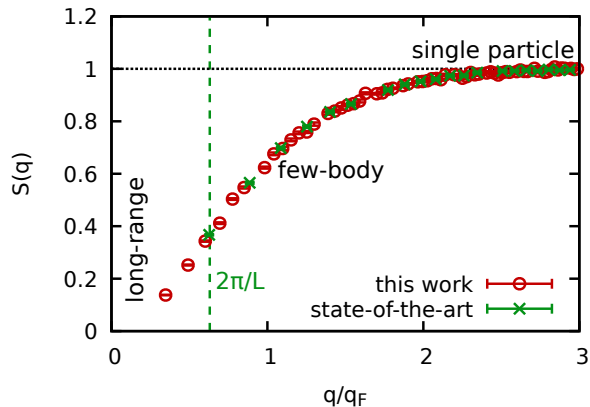


Table of Contents (TOC)/Abstract graphic.

The accurate description of fermionic quantum many-body systems is a paramount task within physics, quantum chemistry, material science, and related fields. An important subcategory is given by thermal simulations that describe quantum systems at finite temperatures. For example, warm dense matter (WDM),¹ an extreme state combining high temperatures ($T \sim 10^4 - 10^8$ K), densities ($n \sim 10^{22} - 10^{27}$ cm⁻³) and pressures ($P \sim 1 - 10^4$ GBar), is ubiquitous throughout our universe and occurs in a host of astrophysical objects such as giant planet interiors² and brown dwarfs.^{3,4} In addition, the fuel capsule in inertial confinement fusion applications has to traverse the WDM regime⁵ in a controlled way to reach ignition.⁶ Consequently, WDM constitutes a highly active topic and is routinely realized in experiments at large research facilities using different techniques.⁷ Other examples for thermal quantum many-body systems of fermions include ultracold atoms⁸⁻¹² and electrons in quantum dots.¹³⁻¹⁶

From a theoretical perspective, the rigorous description of such systems constitutes a difficult challenge as it must capture the complex interplay of effects such as non-ideality,

quantum degeneracy and diffraction, as well as strong thermal excitations.^{1,17} In this context, the *ab initio* path integral Monte Carlo (PIMC) method¹⁸ is a promising candidate as it is, in principle, capable to deliver an exact solution to the full quantum many-body problem of interest without the need for empirical input such as the exchange–correlation functional in density functional theory¹⁹ or the self-energy in Green function approaches.^{20,21} Unfortunately, the PIMC simulation of fermions is afflicted with the notorious fermion sign problem,²² which leads to an exponential increase in the required compute time for example upon increasing the system size N .^{23,24}

While a complete solution of the sign problem remains unlikely, the pressing need for an accurate description of quantum Fermi systems has ignited a number of promising developments in the field of quantum Monte Carlo simulations over the last decade, e.g. Refs.^{25–40} On the one hand, these methods allow for a very accurate description of a given N -body system. In combination with appropriate finite-size corrections,^{31,41,42} this has led to the first reliable parametrizations of the uniform electron gas (UEG) covering the entire WDM parameter space,^{32,40,43,44} allowing for thermal DFT calculations of real WDM systems on the level of the local density approximation^{45–47} and beyond.^{48,49} On the other hand, these tools by themselves are not capable to capture long-range phenomena⁵⁰ that manifest on length scales larger than the given box length L which, for a given density, is determined by the number of simulated particles N .

This precludes, for example, the description of X-ray Thomson scattering (XRTS) experiments, a key diagnostic for WDM applications,^{51–54} in a forward scattering geometry where the system is probed at a small momentum transfer q and, consequently, a long wavelength $\lambda = 2\pi/q$. Moreover, electrical⁵⁵ and thermal⁵⁶ conductivities are necessarily defined in the optical limit of $q \rightarrow 0$, which makes the simulation of large systems even more important.

Very recently, Xiong and Xiong⁵⁷ have proposed to alleviate the sign problem by carrying out path integral molecular dynamics (PIMD) simulations of fictitious identical particles governed by the continuous parameter $\xi \in [-1, 1]$, with $\xi = 1$, $\xi = 0$, and $\xi = -1$ correspond-

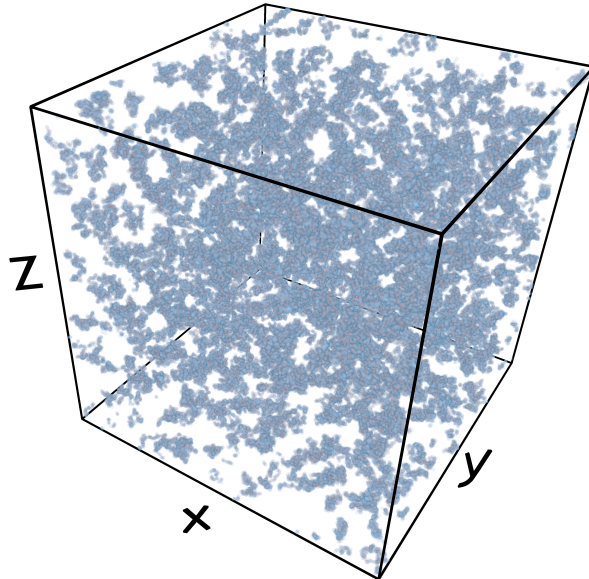


Figure 1: Snapshot from an *ab initio* PIMC simulation of the warm dense UEG at $r_s = 2$ and $\Theta = 1$ with $N = 1000$ unpolared electrons. Each electron is represented by an entire path along the imaginary time with $P = 200$ time-steps (blue spheres); their extension corresponds to the thermal wavelength $\lambda_\beta = \sqrt{2\pi\hbar^2\beta/m_e}$ and takes into account quantum effects such as diffraction.

ing to the physically relevant cases of Bose-, Boltzmann-, and Fermi-statistics, respectively. Subsequently, Dornheim *et al.*⁵⁸ have implemented the same idea into PIMC and found that it works remarkably well for weakly to moderately quantum degenerate systems, including the warm dense UEG. In a nutshell, these findings imply the intriguing possibility of PIMC simulations of large Fermi systems without the exponential bottleneck due to the sign problem.

In the present work, we rigorously test this hypothesis by carrying out unprecedented large-scale PIMC simulations (with $N \leq 10^3$, see Fig. 1) of the UEG both at WDM parameters, and in the strongly coupled electron liquid regime.^{59,60} In this way, we unambiguously demonstrate the capability of the ξ -extrapolation method to accurately describe the system on all length scales, including the difficult long-wavelength limit of $q \rightarrow 0$.

These findings open up a gamut of new possibilities to study WDM, ultracold atoms, and a host of other Fermi systems.

Path integral Monte Carlo and the ξ -extrapolation method. Let us consider a system of $N = N^\uparrow + N^\downarrow$ unpolarized electrons in a cubic simulation cell of volume $V = L^3$ at an inverse temperature $\beta = 1/k_B T$. Writing the partition function in coordinate representation then gives

$$Z_{N,V,\beta} = \frac{1}{N^\uparrow! N^\downarrow!} \sum_{\sigma_{N^\uparrow} \in S_{N^\uparrow}} \sum_{\sigma_{N^\downarrow} \in S_{N^\downarrow}} \xi^{N_{\text{pp}}} \int_V d\mathbf{R} \langle \mathbf{R} | e^{-\beta \hat{H}} | \hat{\pi}_{\sigma_{N^\uparrow}} \hat{\pi}_{\sigma_{N^\downarrow}} \mathbf{R} \rangle, \quad (1)$$

where the meta-variable $\mathbf{R} = (\mathbf{r}_1, \dots, \mathbf{r}_N)^T$ contains the coordinates of both spin-up and spin-down electrons. Due to the indistinguishable nature of electrons of equal spin-orientation, we have to sum over all possible permutations of particle coordinates that are realized by the corresponding permutation operators $\hat{\pi}_{\sigma_{N^i}}$ with $i \in \{\uparrow, \downarrow\}$. A special role is played by the aforementioned continuous spin-variable ξ , which effectively controls the likelihood of pair exchanges (with N_{pp} being the particular number of pair exchanges needed to realize a particular permutation) in the PIMC simulation.^{58,61} For $\xi \geq 0$, all contributions to Z are positive, and no sign problem occurs. In contrast, positive and negative contributions increasingly cancel for $\xi < 0$, which is most severe in the fermionic limit of $\xi = -1$. To avoid the associated exponential decrease in the accuracy, Xiong and Xiong⁵⁷ have proposed to extrapolate to the latter by fitting a quadratic polynomial of the form

$$O(\xi) = a_O + b_O \xi + c_O \xi^2 \quad (2)$$

to PIMC results for an observable \hat{O} in the sign-problem free domain, i.e., $\xi \geq 0$. Subsequently, Dornheim *et al.*⁵⁸ have found that this approach works remarkably well for a host of observables, including the energy E , static structure factor $S(q)$, and even the imaginary-time density–density correlation function $F(q, \tau)$.^{54,62}

Additional details regarding the derivation of the imaginary-time PIMC method¹⁸ as well as the fermion sign problem^{23,24} have been presented in the literature and need not be repeated here. For completeness, we note that we use a canonical adaption of the worm

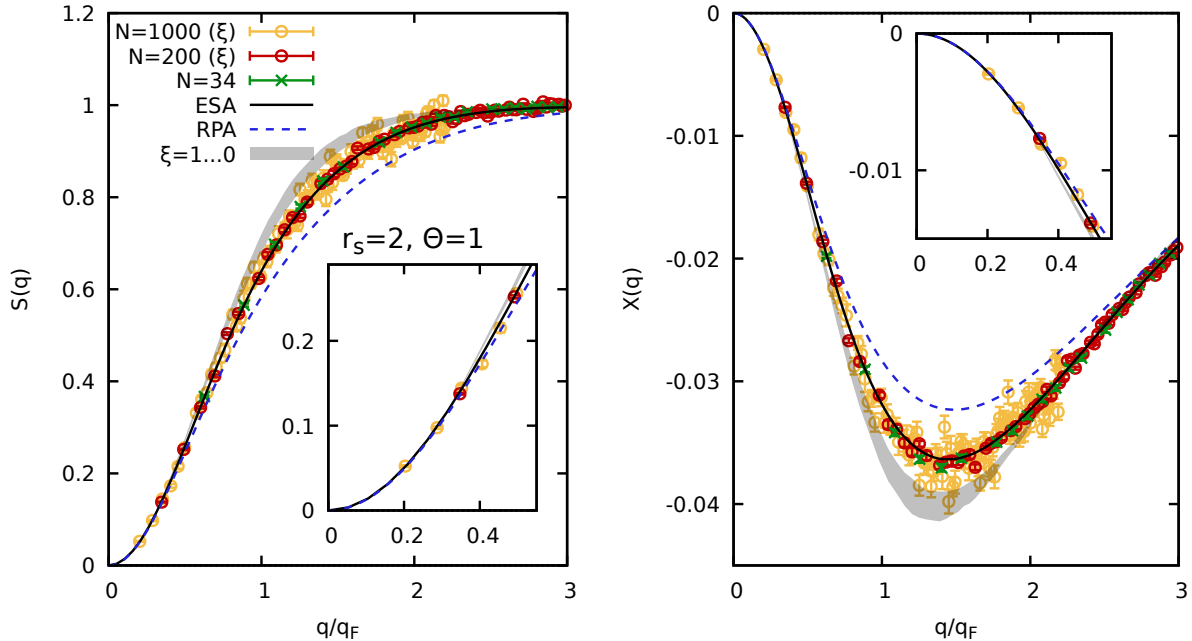


Figure 2: PIMC simulation of the warm dense UEG at $r_s = 2$ and $\Theta = 1$. Left: Static structure factor $S(q)$; right: static linear density response function $\chi(q)$ [see Eq. (3)]. Dashed blue: random phase approximation (RPA); solid black: semi-empirical *effective static approximation* (ESA);^{66,67} green crosses: exact PIMC results for $N = 34$; red circles (yellow stars): new ξ -extrapolated PIMC results for $N = 200$ ($N = 1000$). The insets show magnified segments around the long-wavelength limit.

algorithm by Boninsegni *et al.*^{63,64} based on the extended ensemble idea presented in Ref.⁶⁵ All results have been obtained for $P = 200$ imaginary-time propagators with a primitive factorization scheme, and the convergence with P has been carefully checked.

Results. Let us start our investigation by considering the UEG at a Wigner-Seitz radius of $r_s = 2$ and degeneracy temperature $\Theta = k_B T / E_F = 1$ (where E_F is the usual Fermi energy⁶⁸). This corresponds to a metallic density that can be realized for example in experiments with aluminium⁶⁹ at the electronic Fermi temperature of $T = 12.53$ eV. In the left panel of Fig. 2, we show our new results for the static structure factor $S(q)$. More specifically, the dashed blue curve corresponds to the well-known random phase approximation (RPA), where the electronic density response to an external perturbation is treated on a mean-field level.^{54,68} For the case of the UEG, the RPA becomes exact in the long-wavelength limit of $q \rightarrow 0$, but systematically underestimates the true SSF around the Fermi wavenumber

$q \sim q_F$. These shortcomings have been corrected in the semi-empirical *effective static approximation* (ESA),^{66,67} which is shown as the solid black line, and which is expected to give a highly accurate description of the UEG over the entire q -range at these conditions. This is indeed verified by the green crosses depicting exact PIMC results for $S(q)$ that have been obtained based on simulations with $N = 34$ electrons without the ξ -extrapolation method. Alas, these data are only available above a minimum wavenumber of $q_{\min} = 0.63q_F$ which is defined by the size of the simulation cell.³¹

To overcome this limitation, we have carried out extensive new calculations with $N = 200$ and $N = 1000$ electrons using the method explored in Refs.^{57,58} In Fig. 1, we show a snapshot from a corresponding PIMC calculation with $N = 1000$. A particular strength of the method is the full treatment of quantum diffraction effects over the entire length scale, as each electron is represented by an entire path of $P = 200$ positions along the imaginary-time domain; these paths would collapse to point particles in the classical limit of $\beta \rightarrow 0$.

Coming back to the SSF shown in Fig. 2, we find that the new results for $N = 200$ (red circles) and $N = 1000$ (yellow circles) that have been obtained based on Eq. (2) using input data from the sign-problem free domain of $\xi \geq 0$ (shaded grey area) are in excellent agreement with the ESA results and the exact PIMC results for $N = 34$, where they are available. In particular, we unambiguously demonstrate that this approach is capable to recover the $q \rightarrow 0$ limit, which is known exactly in the case of the UEG; see also the inset showing a magnified segment around this regime. The somewhat larger spread of the data points for the $N = 200$ and $N = 1000$ cases is due to the computational cost increasing with $\sim N^2$ and thus the significantly reduced number of snapshots available for averaging with manageable computational cost.

In the right panel of Fig. 2, we repeat this analysis for the static linear density response function $\chi(q)$, which can be computed from PIMC results for the ITCF $F(q, \tau)$ based on the

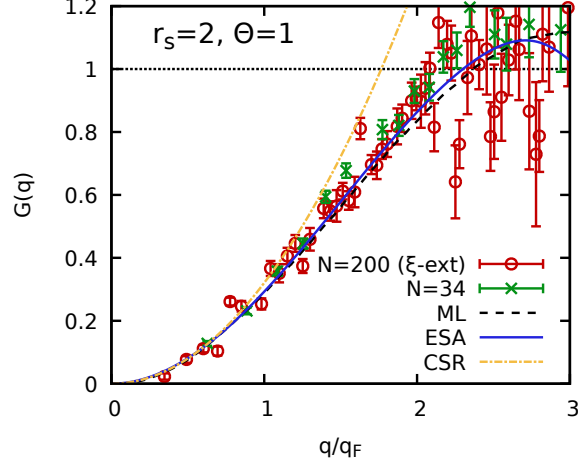


Figure 3: Local field correction $G(q)$ [see Eq. (4)] for $r_s = 2$ and $\Theta = 1$. Dashed black: neural-net representation from Ref.;⁷¹ solid blue: analytical parametrization of the ESA;⁶⁷ dash-dotted yellow: compressibility sum-rule [Eq. (5)] evaluated from the parametrization by Groth *et al.*;³² green crosses: exact PIMC results for $N = 34$; red circles: new ξ -extrapolated PIMC results for $N = 200$.

imaginary-time version of the well-known fluctuation–dissipation theorem^{62,70}

$$\chi(q) = -\frac{N}{V} \int_0^\beta d\tau F(q, \tau) \quad . \quad (3)$$

Overall, we find the same general trends as for $S(q)$: the RPA underestimates the true magnitude of the density response around the Fermi wavenumber; the ESA is quasi-exact for all q and nicely agrees with the direct PIMC results; most importantly, our new, large-scale PIMC simulations are capable to predict the correct $q \rightarrow 0$ limit, see also the inset.

To further highlight the high quality of these results, we consider the exact expression

$$\chi(q) = \frac{\chi_0(q)}{1 - \frac{4\pi}{q^2} [1 - G(q)] \chi_0(q)} \quad , \quad (4)$$

where $\chi_0(q)$ is the temperature-dependent Lindhard function describing the density response of an ideal Fermi gas⁶⁸ and the complete, wavenumber resolved, information about electronic exchange–correlation effects is included in the static local field correction (LFC) $G(q)$.^{71,72} Therefore, the LFC constitutes key input for a number of applications, such as the computa-

tion of electrical conductivities,⁷³ the interpretation of XRTS experiments,⁷⁴ the development of thermal XC functionals,^{75–78} and as the exchange–correlation kernel in time-dependent DFT simulations.^{79,80} In Fig. 3, we show the LFC for the same conditions as in Fig. 2. The solid blue line corresponds to the recent analytical parametrization of the ESA⁶⁷ that includes the correct $q \rightarrow 0$ limit given by the compressibility sum-rule (CSR),

$$\lim_{q \rightarrow 0} G(q) = -\frac{q^2}{4\pi} \frac{\partial^2}{\partial n^2} (n f_{\text{xc}}) , \quad (5)$$

where f_{xc} is the exchange–correlation energy of the UEG.^{32,40,43,44} In practice, we evaluate Eq. (5) using the parametrization by Groth *et al.*,³² and the results are included as the dash-dotted yellow curve. Furthermore, the dashed black line shows the PIMC based neural net representation of $G(q; r_s, \Theta)$ from Ref.⁷¹ The ESA and ML curves are very similar in the depicted q -range and only noticeably differ in the single-particle limit of $q \gg q_{\text{F}}$. As usual, the green crosses show exact PIMC results for $N = 34$ that have been obtained by inverting Eq. (4), and the red circles the corresponding ξ -extrapolated PIMC results for $N = 200$. Again, we find that the ξ -extrapolation method very accurately describes this sophisticated exchange–correlation property over all length scales. This raises the intriguing possibility to study long-range correlations in other Fermi systems such as warm dense hydrogen, where the true $q \rightarrow 0$ limit is a subject of active investigations.^{50,55,81}

As a second example, we consider the UEG at $r_s = 10$ and $\Theta = 0.5$. These conditions correspond to the boundary of the strongly coupled electron liquid regime^{59,60} that is known to exhibit a wealth of interesting physical phenomena such as a non-monotonic roton-type feature in the dynamic structure factor.^{31,53,82–84} In Fig. 4, we show the corresponding SSF and static linear response function with the usual color code. To assess the accuracy of the ξ -extrapolation at these conditions, we have carried out new, exact PIMC simulations for $N = 14$ electrons (green crosses). We find an average sign of $S = 0.02$, making them computationally involved, but still feasible.²³ Considering the static structure factor, the

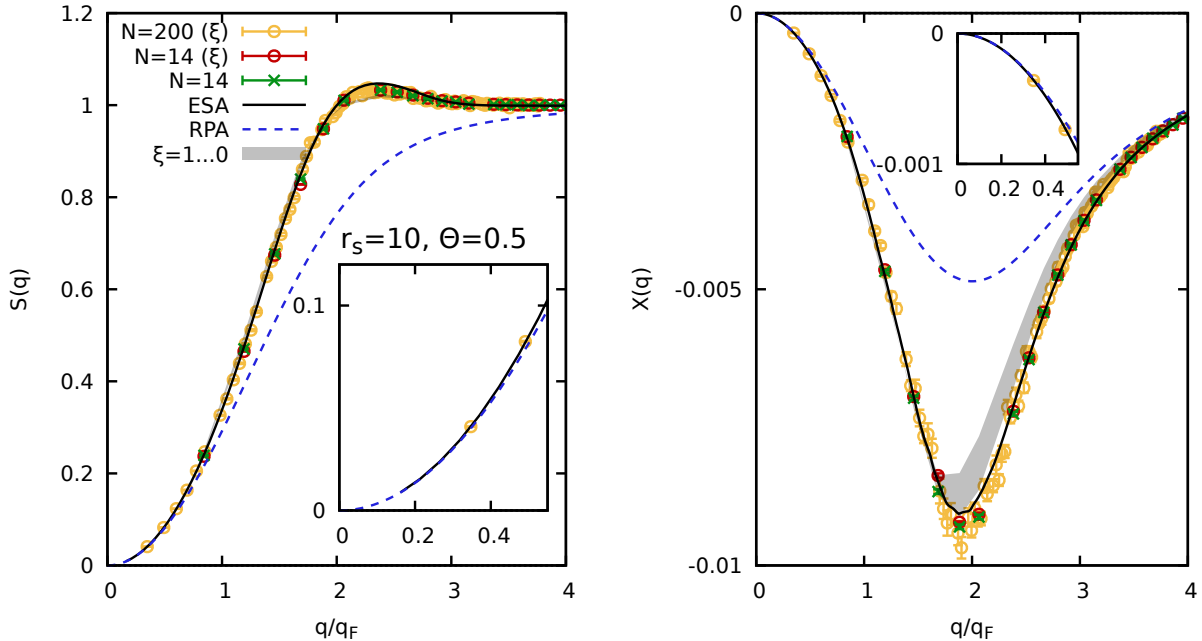


Figure 4: PIMC simulation of the warm dense UEG at $r_s = 10$ and $\Theta = 0.5$. Left: Static structure factor $S(q)$; right: static linear density response function $\chi(q)$ [see Eq. (3)]. Dashed blue: random phase approximation (RPA); solid black: semi-empirical *effective static approximation* (ESA);^{66,67} green crosses: exact PIMC results for $N = 14$; red and yellow circles: ξ -extrapolated PIMC results for $N = 14$ and $N = 200$. The insets show magnified segments around the long-wavelength limit.

PIMC reference results are in very good agreement with the ESA curve; small systematic deviations are only visible in the vicinity of the peak where the latter slightly overestimates the true SSF. The red circles show the ξ -extrapolated results, which nicely agree with the green crosses everywhere. Interestingly, we find that the effect of quantum statistics on $S(q)$ is small (see the shaded grey area indicating the sign-problem free domain of $\xi \geq 0$), even though the degree of cancellations of positive and negative terms is substantial already for the relatively small system size of $N = 14$. A similar observation has been reported recently for the case of ultracold ^3He ,¹¹ which, too, constitutes a strongly coupled quantum liquid. Finally, the yellow circles show new, ξ -extrapolated results for $N = 200$ electrons, and we find the same good performance as for the case of $r_s = 2$ investigated above.

In the right panel of Fig. 4, we show results for the static linear density response function $\chi(q)$. First, we observe that the impact of quantum statistics is considerably larger than

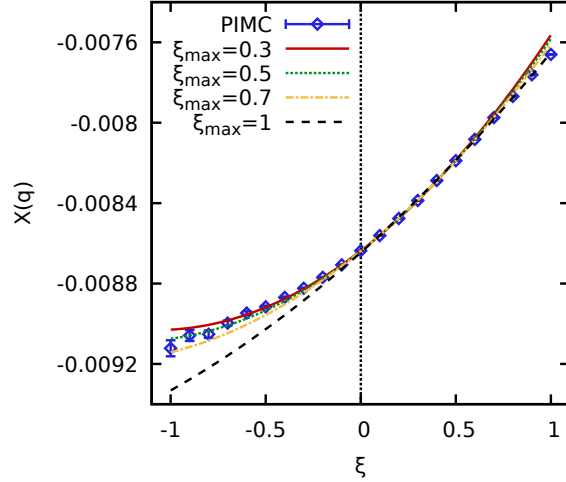


Figure 5: ξ -dependence of the static linear density response function $\chi(q)$ for $N = 14$, $r_s = 10$, and $\Theta = 0.5$ at $q \approx 2q_F$. The blue diamonds depict the exact PIMC results and the various curves have been obtained by quadratic fits based on Eq. (2) using as input data in the interval of $\xi \in [0, \xi_{\max}]$.

for $S(q) = F(q, 0)$. Indeed, Eq. (3) implies that $\chi(q)$ directly depends on the imaginary-time diffusion of the electrons, which is more sensitive to quantum effects compared to the static structure of the system. Second, we find that the ξ -extrapolation based on Eq. (2) becomes somewhat inaccurate when the full sign-problem free interval of $\xi \in [0, 1]$ is used. This is investigated in more detail in Fig. 5, where we show the ξ -dependence of $\chi(q)$ at $q \approx 2q_F$. Specifically, the blue diamonds show exact PIMC results, which are available as a benchmark over the full ξ -range in this case, and the various curves correspond to quadratic extrapolations based on Eq. (2) using as input data within different intervals $\xi \in [0, \xi_{\max}]$. The dashed black line corresponds to the usual choice of $\xi_{\max} = 1$ and underestimates the true density response in the fermionic limit of $\xi = -1$ by about 1%. We note that this is still a reasonable level of accuracy for the description of a strongly coupled Fermi liquid, but it is considerably worse compared to the WDM case investigated above. The dash-dotted yellow and dotted green curves correspond to $\xi_{\max} = 0.7$ and $\xi_{\max} = 0.5$, respectively, and exhibit a substantially improved agreement with the PIMC data for $\xi < 0$. Empirically, these values of ξ seem equally reasonable and we have used $\xi = 0.5$ to compute the red circles in the right panel of Fig. 4. Evidently, this truncated extrapolation scheme works very well over the

entire q -range. Finally, the solid red curve in Fig. 5 corresponds to $\xi_{\max} = 0.3$. In this case, the ξ -extrapolation is based on only four data points, which leads to a larger uncertainty compared to the other analyzed fitting intervals.

Returning to the static linear density response function shown in Fig. 4, we find that the effect of quantum statistics is restricted to the range of $1.75q_F \lesssim q \lesssim 4q_F$ for these conditions. Unsurprisingly, the ξ -extrapolated results for $N = 200$ electrons (yellow circles) are in excellent agreement with the solid black ESA curve everywhere, and reproduce the correct $q \rightarrow 0$ limit, see also the inset. We thus conclude that the ξ -extrapolation method is applicable beyond the WDM regime, and constitutes a valuable tool for the investigation of strongly coupled Fermi liquids.

Summary and outlook. In this work, we have presented extensive new *ab initio* PIMC simulations of the UEG with unprecedented system size ($N \leq 1000$ electrons). In this way, we have unambiguously demonstrated that the ξ -extrapolation method^{57,58} is capable to describe non-ideal Fermi systems over all length scales, including the long-range limit ($q \rightarrow 0$) that is known exactly in the case of the UEG, but not for other systems such as warm dense two-component plasmas or ultracold atoms. From a physical perspective, we have considered both the WDM regime that is of high current interest e.g. for the description of laser fusion applications and astrophysical models, and the strongly coupled electron liquid regime, which exhibits phenomena such as the roton-type feature of the dynamic structure factor that is interesting in itself. We are convinced that these findings open up a host of new avenues for impactful future research in a great variety of research fields.

First, an intriguing application of the ξ -extrapolation method stems from its unique capability to accurately probe even the largest length scales of the UEG. Naturally, when approaching the long-wavelength limit, otherwise inaccessible information is unlocked that concerns specific thermodynamic quantities as well as transport coefficients. (a) The $q \rightarrow 0$ limit of the static local field correction directly leads to the isothermal compressibility via the eponymous sum rule without the need for thermodynamic integration or differentia-

tions.⁶⁸ Such a thermodynamic route that is independent from the internal energy would provide a rigorous check for existing UEG equations of state^{32,44} which are typically free energy representations whose derived thermodynamic properties are known to suffer from certain pathologies.⁴⁸ (b) The frequency dependent electrical conductivity is connected to the long-wavelength limit of the current response function, while the thermal conductivity is connected to the hydrodynamic limit of the heat (or energy) current response function, see the respective Kubo and Green-Kubo formulas.^{85,86} (c) Within the current density version of linear response theory, it is known that the generalized visco-elastic coefficients are connected to long-wavelength limits that involve the respective longitudinal and transverse dynamic local field corrections.^{87,88} Moreover, the shear viscosity is connected to a hydrodynamic limit that involves the transverse local field correction.^{68,87,88} (d) Within the spin resolved density version of linear response theory, it is known that the static spin susceptibility is connected to the $q \rightarrow 0$ limit of the static spin-antisymmetric local field correction.⁸⁹ In addition, the spin diffusion coefficient/constant is connected to a hydrodynamic limit that involves the dynamic spin-antisymmetric local field correction.⁸⁵

More important, the ξ -extrapolation method will allow for the first time to study long-range phenomena in real WDM systems based on *ab initio* PIMC simulations starting with hydrogen.⁹⁰⁻⁹⁴ This will facilitate the interpretation of XRTS experiments in a forward scattering geometry where the system is effectively probed on large length scales. From a physical perspective, one can expect that such measurements will be highly sensitive to the density of the probed system, and, in this way, will complement backward scattering measurements that are particularly sensitive to parameters such as the temperature and ionization.⁹⁵⁻⁹⁷ In accordance with the above reasoning, a second potential application of the ξ -extrapolation method that is related to the study of WDM concerns the estimation of thermodynamic quantities and transport coefficients such as the thermal conductivity⁵⁶ and the electrical conductivity,⁵⁵ which may substantially depend on exchange-correlation effects.⁵⁰

Returning to the UEG itself, it might be interesting to study the spin-resolved density

response, as well as the spin-resolved components of the static structure factor which, in contrast to the spin-averaged $\chi(q)$ and $S(q)$, are not described properly by the RPA or by more sophisticated dielectric schemes^{98–104} even in the long-range limit of $q \rightarrow 0$.¹⁰⁵ Such a study might give new insights into the performance of different approximations to the LFC, and can provide useful input and benchmark data for other applications.

A further interesting line of research is given by the application of the ξ -extrapolation method to other systems. Based on our encouraging results for the strongly coupled electron liquid, we propose to utilize the method to ultracold atoms such as the short-range interacting ^3He , but also dipolar systems.^{23,106} For these systems, interesting long-range phenomena include the acoustic mode in the dynamic structure factor for small q , and the long-wavelength limit of the SSF that is given by the compressibility sum-rule.¹⁰⁷ Furthermore, we note that the method has already been applied to electrons in quantum dots in previous studies.^{57,58,108} Indeed, it is well known that trapped Fermi systems exhibit interesting effects such as the formation of Wigner molecules^{109,110} and a negative superfluid fraction.^{16,106,111}

Finally, we stress that, despite its impressive performance, the ξ -extrapolation method is a very new technique, and its further methodological improvement remains in its infancy compared to more established methods such as restricted PIMC.^{25,112,113} The observed improvement of the extrapolation due to the truncation of the ξ -interval in the sign-problem free domain for $r_s = 10$ and $\Theta = 0.5$ suggests that much can potentially be gained by developing better extrapolation schemes. In addition, the absence of the exponential bottleneck poses new challenges, which might be met by combining PIMC with other ideas such as the adaptive long-range potential scheme that has been suggested in the recent Ref.,¹¹⁴ or the quantum ring-polymer contraction method that has been introduced in the context of PIMD.¹¹⁵

Acknowledgments

This work was partially supported by the Center for Advanced Systems Understanding (CASUS) which is financed by Germany's Federal Ministry of Education and Research (BMBF) and by the Saxon state government out of the State budget approved by the Saxon State Parliament. This work has received funding from the European Research Council (ERC) under the European Union's Horizon 2022 research and innovation programme (Grant agreement No. 101076233, "PREXTREME"). The PIMC calculations were partly carried out at the Norddeutscher Verbund für Hoch- und Höchstleistungsrechnen (HLRN) under grant mvp00024, on a Bull Cluster at the Center for Information Services and High Performance Computing (ZIH) at Technische Universität Dresden, and on the HoreKa supercomputer funded by the Ministry of Science, Research and the Arts Baden-Württemberg and by the Federal Ministry of Education and Research.

References

- (1) Graziani, F., Desjarlais, M. P., Redmer, R., Trickey, S. B., Eds. Frontiers and Challenges in Warm Dense Matter; Springer: International Publishing, 2014.
- (2) Benuzzi-Mounaix, A.; Mazevet, S.; Ravasio, A.; Vinci, T.; Denoëud, A.; Koenig, M.; Amadou, N.; Brambrink, E.; Festa, F.; Levy, A.; Harmand, M.; Brygoo, S.; Huser, G.; Recoules, V.; Bouchet, J.; Morard, G.; Guyot, F.; de Resseguier, T.; Myanishi, K.; Ozaki, N.; Dorchies, F.; Gaudin, J.; Leguay, P. M.; Peyrusse, O.; Henry, O.; Raffestin, D.; Pape, S. L.; Smith, R.; Musella, R. Progress in warm dense matter study with applications to planetology. Phys. Scripta **2014**, T161, 014060.
- (3) Becker, A.; Lorenzen, W.; Fortney, J. J.; Nettelmann, N.; Schöttler, M.; Redmer, R. Ab initio equations of state for hydrogen (H-REOS.3) and helium (He-REOS.3) and

- their implications for the interior of brown dwarfs. *Astrophys. J. Suppl. Ser* **2014**, 215, 21.
- (4) Saumon, D.; Hubbard, W. B.; Chabrier, G.; van Horn, H. M. The role of the molecular-metallic transition of hydrogen in the evolution of Jupiter, Saturn, and brown dwarfs. *Astrophys. J* **1992**, 391, 827–831.
- (5) Hu, S. X.; Militzer, B.; Goncharov, V. N.; Skupsky, S. First-principles equation-of-state table of deuterium for inertial confinement fusion applications. *Phys. Rev. B* **2011**, 84, 224109.
- (6) Betti, R.; Hurricane, O. A. Inertial-confinement fusion with lasers. *Nature Physics* **2016**, 12, 435–448.
- (7) Falk, K. Experimental methods for warm dense matter research. *High Power Laser Sci. Eng* **2018**, 6, e59.
- (8) Giorgini, S.; Pitaevskii, L. P.; Stringari, S. Theory of ultracold atomic Fermi gases. *Rev. Mod. Phys.* **2008**, 80, 1215–1274.
- (9) Ceperley, D. M. Path-integral calculations of normal liquid ^3He . *Phys. Rev. Lett.* **1992**, 69, 331–334.
- (10) Godfrin, H.; Meschke, M.; Lauter, H.-J.; Sultan, A.; Böhm, H. M.; Krotscheck, E.; Panholzer, M. Observation of a roton collective mode in a two-dimensional Fermi liquid. *Nature* **2012**, 483, 576–579.
- (11) Dornheim, T.; Moldabekov, Z. A.; Vorberger, J.; Militzer, B. Path integral Monte Carlo approach to the structural properties and collective excitations of liquid ^3He without fixed nodes. *Scientific Reports* **2022**, 12, 708.
- (12) Filinov, A. V.; Ara, J.; Tkachenko, I. M. Dynamic properties and the roton mode

- attenuation in the liquid ^3He : an ab initio study within the self-consistent method of moments. Phil. Trans. R. Soc. A **2023**, 381, 20220324.
- (13) Reimann, S. M.; Manninen, M. Electronic structure of quantum dots. Rev. Mod. Phys. **2002**, 74, 1283–1342.
- (14) Weiss, S.; Egger, R. Path-integral Monte Carlo simulations for interacting few-electron quantum dots with spin-orbit coupling. Phys. Rev. B **2005**, 72, 245301.
- (15) Kylänpää, I.; Räsänen, E. Path integral Monte Carlo benchmarks for two-dimensional quantum dots. Phys. Rev. B **2017**, 96, 205445.
- (16) Dornheim, T.; Yan, Y. Abnormal quantum moment of inertia and structural properties of electrons in 2D and 3D quantum dots: an ab initio path-integral Monte Carlo study. New Journal of Physics **2022**, 24, 113024.
- (17) Bonitz, M.; Dornheim, T.; Moldabekov, Z. A.; Zhang, S.; Hamann, P.; Kählert, H.; Filinov, A.; Ramakrishna, K.; Vorberger, J. Ab initio simulation of warm dense matter. Physics of Plasmas **2020**, 27, 042710.
- (18) Ceperley, D. M. Path integrals in the theory of condensed helium. Rev. Mod. Phys. **1995**, 67, 279.
- (19) Jones, R. O. Density functional theory: Its origins, rise to prominence, and future. Rev. Mod. Phys. **2015**, 87, 897–923.
- (20) Stefanucci, G.; van Leeuwen, R. Nonequilibrium Many-Body Theory of Quantum Systems: A Modern Introduction; Cambridge University Press, 2013.
- (21) Schlünzen, N.; Hermanns, S.; Scharnke, M.; Bonitz, M. Ultrafast dynamics of strongly correlated fermions—nonequilibrium Green functions and selfenergy approximations. Journal of Physics: Condensed Matter **2019**, 32, 103001.

- (22) Troyer, M.; Wiese, U. J. Computational Complexity and Fundamental Limitations to Fermionic Quantum Monte Carlo Simulations. Phys. Rev. Lett **2005**, 94, 170201.
- (23) Dornheim, T. Fermion sign problem in path integral Monte Carlo simulations: Quantum dots, ultracold atoms, and warm dense matter. Phys. Rev. E **2019**, 100, 023307.
- (24) Dornheim, T. Fermion sign problem in path integral Monte Carlo simulations: grand-canonical ensemble. Journal of Physics A: Mathematical and Theoretical **2021**, 54, 335001.
- (25) Brown, E. W.; Clark, B. K.; DuBois, J. L.; Ceperley, D. M. Path-Integral Monte Carlo Simulation of the Warm Dense Homogeneous Electron Gas. Phys. Rev. Lett. **2013**, 110, 146405.
- (26) Blunt, N. S.; Rogers, T. W.; Spencer, J. S.; Foulkes, W. M. C. Density-matrix quantum Monte Carlo method. Phys. Rev. B **2014**, 89, 245124.
- (27) Schoof, T.; Groth, S.; Vorberger, J.; Bonitz, M. Ab Initio Thermodynamic Results for the Degenerate Electron Gas at Finite Temperature. Phys. Rev. Lett. **2015**, 115, 130402.
- (28) Dornheim, T.; Groth, S.; Filinov, A.; Bonitz, M. Permutation blocking path integral Monte Carlo: a highly efficient approach to the simulation of strongly degenerate non-ideal fermions. New Journal of Physics **2015**, 17, 073017.
- (29) Malone, F. D.; Blunt, N. S.; Shepherd, J. J.; Lee, D. K. K.; Spencer, J. S.; Foulkes, W. M. C. Interaction picture density matrix quantum Monte Carlo. The Journal of Chemical Physics **2015**, 143, 044116.
- (30) Malone, F. D.; Blunt, N. S.; Brown, E. W.; Lee, D. K. K.; Spencer, J. S.; Foulkes, W. M. C.; Shepherd, J. J. Accurate Exchange-Correlation Energies for the Warm Dense Electron Gas. Phys. Rev. Lett. **2016**, 117, 115701.

- (31) Dornheim, T.; Groth, S.; Sjostrom, T.; Malone, F. D.; Foulkes, W. M. C.; Bonitz, M. Ab Initio Quantum Monte Carlo Simulation of the Warm Dense Electron Gas in the Thermodynamic Limit. Phys. Rev. Lett. **2016**, 117, 156403.
- (32) Groth, S.; Dornheim, T.; Sjostrom, T.; Malone, F. D.; Foulkes, W. M. C.; Bonitz, M. Ab initio Exchange–Correlation Free Energy of the Uniform Electron Gas at Warm Dense Matter Conditions. Phys. Rev. Lett. **2017**, 119, 135001.
- (33) Yilmaz, A.; Hunger, K.; Dornheim, T.; Groth, S.; Bonitz, M. Restricted configuration path integral Monte Carlo. The Journal of Chemical Physics **2020**, 153, 124114.
- (34) Lee, J.; Morales, M. A.; Malone, F. D. A phaseless auxiliary-field quantum Monte Carlo perspective on the uniform electron gas at finite temperatures: Issues, observations, and benchmark study. The Journal of Chemical Physics **2021**, 154, 064109.
- (35) Hunger, K.; Schoof, T.; Dornheim, T.; Bonitz, M.; Filinov, A. Momentum distribution function and short-range correlations of the warm dense electron gas: Ab initio quantum Monte Carlo results. Phys. Rev. E **2021**, 103, 053204.
- (36) Hirshberg, B.; Invernizzi, M.; Parrinello, M. Path integral molecular dynamics for fermions: Alleviating the sign problem with the Bogoliubov inequality. The Journal of Chemical Physics **2020**, 152, 171102.
- (37) Dornheim, T.; Invernizzi, M.; Vorberger, J.; Hirshberg, B. Attenuating the fermion sign problem in path integral Monte Carlo simulations using the Bogoliubov inequality and thermodynamic integration. The Journal of Chemical Physics **2020**, 153, 234104.
- (38) Chin, S. A. High-order path-integral Monte Carlo methods for solving quantum dot problems. Phys. Rev. E **2015**, 91, 031301.
- (39) Dornheim, T.; Groth, S.; Malone, F. D.; Schoof, T.; Sjostrom, T.; Foulkes, W. M. C.;

- Bonitz, M. Ab initio quantum Monte Carlo simulation of the warm dense electron gas. Physics of Plasmas **2017**, 24, 056303.
- (40) Dornheim, T.; Groth, S.; Bonitz, M. The uniform electron gas at warm dense matter conditions. Phys. Reports **2018**, 744, 1–86.
- (41) Holzmann, M.; Clay, R. C.; Morales, M. A.; Tubman, N. M.; Ceperley, D. M.; Pierleoni, C. Theory of finite size effects for electronic quantum Monte Carlo calculations of liquids and solids. Phys. Rev. B **2016**, 94, 035126.
- (42) Dornheim, T.; Vorberger, J. Overcoming finite-size effects in electronic structure simulations at extreme conditions. The Journal of Chemical Physics **2021**, 154, 144103.
- (43) Karasiev, V. V.; Sjostrom, T.; Dufty, J.; Trickey, S. B. Accurate Homogeneous Electron Gas Exchange-Correlation Free Energy for Local Spin-Density Calculations. Phys. Rev. Lett. **2014**, 112, 076403.
- (44) Karasiev, V. V.; Trickey, S. B.; Dufty, J. W. Status of free-energy representations for the homogeneous electron gas. Phys. Rev. B **2019**, 99, 195134.
- (45) Karasiev, V. V.; Calderin, L.; Trickey, S. B. Importance of finite-temperature exchange correlation for warm dense matter calculations. Phys. Rev. E **2016**, 93, 063207.
- (46) Ramakrishna, K.; Dornheim, T.; Vorberger, J. Influence of finite temperature exchange-correlation effects in hydrogen. Phys. Rev. B **2020**, 101, 195129.
- (47) Moldabekov, Z.; Böhme, M.; Vorberger, J.; Blaschke, D.; Dornheim, T. Ab Initio Static Exchange-Correlation Kernel across Jacob’s Ladder without Functional Derivatives. Journal of Chemical Theory and Computation **2023**, 19, 1286–1299.
- (48) Karasiev, V. V.; Dufty, J. W.; Trickey, S. B. Nonempirical Semilocal Free-Energy Density Functional for Matter under Extreme Conditions. Phys. Rev. Lett. **2018**, 120, 076401.

- (49) Kozłowski, J.; Perchak, D.; Burke, K. Generalized Gradient Approximation Made Thermal. 2023.
- (50) Rygg, J. R.; Celliers, P. M.; Collins, G. W. Specific Heat of Electron Plasma Waves. Phys. Rev. Lett. **2023**, 130, 225101.
- (51) Glenzer, S. H.; Redmer, R. X-ray Thomson scattering in high energy density plasmas. Rev. Mod. Phys. **2009**, 81, 1625.
- (52) Kraus, D.; Bachmann, B.; Barbrel, B.; Falcone, R. W.; Fletcher, L. B.; Frydrych, S.; Gamboa, E. J.; Gauthier, M.; Gericke, D. O.; Glenzer, S. H.; Göde, S.; Granados, E.; Hartley, N. J.; Helfrich, J.; Lee, H. J.; Nagler, B.; Ravasio, A.; Schumaker, W.; Vorberger, J.; Döppner, T. Characterizing the ionization potential depression in dense carbon plasmas with high-precision spectrally resolved x-ray scattering. Plasma Phys. Control Fusion **2019**, 61, 014015.
- (53) Dornheim, T.; Moldabekov, Z.; Vorberger, J.; Kählert, H.; Bonitz, M. Electronic pair alignment and roton feature in the warm dense electron gas. Communications Physics **2022**, 5, 304.
- (54) Dornheim, T.; Moldabekov, Z. A.; Ramakrishna, K.; Talias, P.; Baczewski, A. D.; Kraus, D.; Preston, T. R.; Chapman, D. A.; Böhme, M. P.; Döppner, T.; Graziani, F.; Bonitz, M.; Cangi, A.; Vorberger, J. Electronic density response of warm dense matter. Physics of Plasmas **2023**, 30, 032705.
- (55) Röpke, G.; Schörner, M.; Redmer, R.; Bethkenhagen, M. Virial expansion of the electrical conductivity of hydrogen plasmas. Phys. Rev. E **2021**, 104, 045204.
- (56) Jiang, S.; Landen, O. L.; Whitley, H. D.; Hamel, S.; London, R.; Clark, D. S.; Sterne, P.; Hansen, S. B.; Hu, S. X.; Collins, G. W.; Ping, Y. Thermal transport in warm dense matter revealed by refraction-enhanced x-ray radiography with a deep-neural-network analysis. Communications Physics **2023**, 6, 98.

- (57) Xiong, Y.; Xiong, H. On the thermodynamic properties of fictitious identical particles and the application to fermion sign problem. The Journal of Chemical Physics **2022**, 157, 094112.
- (58) Dornheim, T.; Tolias, P.; Groth, S.; Moldabekov, Z. A.; Vorberger, J.; Hirshberg, B. Fermionic physics from ab initio path integral Monte Carlo simulations of fictitious identical particles. The Journal of Chemical Physics **2023**, 159, 164113.
- (59) Dornheim, T.; Sjostrom, T.; Tanaka, S.; Vorberger, J. Strongly coupled electron liquid: Ab initio path integral Monte Carlo simulations and dielectric theories. Phys. Rev. B **2020**, 101, 045129.
- (60) Dornheim, T.; Groth, S.; Vorberger, J.; Bonitz, M. Ab initio Path Integral Monte Carlo Results for the Dynamic Structure Factor of Correlated Electrons: From the Electron Liquid to Warm Dense Matter. Phys. Rev. Lett. **2018**, 121, 255001.
- (61) Dornheim, T.; Groth, S.; Filinov, A. V.; Bonitz, M. Path integral Monte Carlo simulation of degenerate electrons: Permutation-cycle properties. The Journal of Chemical Physics **2019**, 151, 014108.
- (62) Dornheim, T.; Moldabekov, Z.; Tolias, P.; Böhme, M.; Vorberger, J. Physical insights from imaginary-time density–density correlation functions. Matter Radiat. Extremes **2023**, 8, 056601.
- (63) Boninsegni, M.; Prokofev, N. V.; Svistunov, B. V. Worm algorithm and diagrammatic Monte Carlo: A new approach to continuous-space path integral Monte Carlo simulations. Phys. Rev. E **2006**, 74, 036701.
- (64) Boninsegni, M.; Prokofev, N. V.; Svistunov, B. V. Worm Algorithm for Continuous-Space Path Integral Monte Carlo Simulations. Phys. Rev. Lett **2006**, 96, 070601.

- (65) Dornheim, T.; Böhme, M.; Militzer, B.; Vorberger, J. Ab initio path integral Monte Carlo approach to the momentum distribution of the uniform electron gas at finite temperature without fixed nodes. Phys. Rev. B **2021**, 103, 205142.
- (66) Dornheim, T.; Cangi, A.; Ramakrishna, K.; Böhme, M.; Tanaka, S.; Vorberger, J. Effective Static Approximation: A Fast and Reliable Tool for Warm-Dense Matter Theory. Phys. Rev. Lett. **2020**, 125, 235001.
- (67) Dornheim, T.; Moldabekov, Z. A.; Tolias, P. Analytical representation of the local field correction of the uniform electron gas within the effective static approximation. Phys. Rev. B **2021**, 103, 165102.
- (68) Giuliani, G.; Vignale, G. Quantum Theory of the Electron Liquid; Cambridge University Press: Cambridge, 2008.
- (69) Ramakrishna, K.; Cangi, A.; Dornheim, T.; Baczewski, A.; Vorberger, J. First-principles modeling of plasmons in aluminum under ambient and extreme conditions. Phys. Rev. B **2021**, 103, 125118.
- (70) Bowen, C.; Sugiyama, G.; Alder, B. J. Static Dielectric Response of the Electron Gas. Phys. Rev. B **1994**, 50, 14838.
- (71) Dornheim, T.; Vorberger, J.; Groth, S.; Hoffmann, N.; Moldabekov, Z.; Bonitz, M. The Static Local Field Correction of the Warm Dense Electron Gas: An ab Initio Path Integral Monte Carlo Study and Machine Learning Representation. J. Chem. Phys. **2019**, 151, 194104.
- (72) Ichimaru, S.; Iyetomi, H.; Tanaka, S. Statistical physics of dense plasmas: Thermodynamics, transport coefficients and dynamic correlations. Physics Reports **1987**, 149, 91–205.

- (73) Veysman, M.; Röpke, G.; Winkel, M.; Reinholz, H. Optical conductivity of warm dense matter within a wide frequency range using quantum statistical and kinetic approaches. Phys. Rev. E **2016**, 94, 013203.
- (74) Fortmann, C.; Wierling, A.; Röpke, G. Influence of local-field corrections on Thomson scattering in collision-dominated two-component plasmas. Phys. Rev. E **2010**, 81, 026405.
- (75) Moldabekov, Z. A.; Lokamani, M.; Vorberger, J.; Cangi, A.; Dornheim, T. Non-empirical Mixing Coefficient for Hybrid XC Functionals from Analysis of the XC Kernel. The Journal of Physical Chemistry Letters **2023**, 14, 1326–1333, PMID: 36724891.
- (76) Moldabekov, Z. A.; Lokamani, M.; Vorberger, J.; Cangi, A.; Dornheim, T. Assessing the accuracy of hybrid exchange-correlation functionals for the density response of warm dense electrons. The Journal of Chemical Physics **2023**, 158, 094105.
- (77) Moldabekov, Z.; Dornheim, T.; Böhme, M.; Vorberger, J.; Cangi, A. The relevance of electronic perturbations in the warm dense electron gas. The Journal of Chemical Physics **2021**, 155, 124116.
- (78) Pribram-Jones, A.; Grabowski, P. E.; Burke, K. Thermal Density Functional Theory: Time-Dependent Linear Response and Approximate Functionals from the Fluctuation-Dissipation Theorem. Phys. Rev. Lett **2016**, 116, 233001.
- (79) Moldabekov, Z. A.; Pavanello, M.; Böhme, M. P.; Vorberger, J.; Dornheim, T. Linear-response time-dependent density functional theory approach to warm dense matter with adiabatic exchange-correlation kernels. Phys. Rev. Res. **2023**, 5, 023089.
- (80) Moldabekov, Z. A.; Vorberger, J.; Lokamani, M.; Dornheim, T. Averaging over atom snapshots in linear-response TDDFT of disordered systems: A case study of warm dense hydrogen. The Journal of Chemical Physics **2023**, 159, 014107.

- (81) Hentschel, T. W.; Kononov, A.; Olmstead, A.; Cangi, A.; Baczewski, A. D.; Hansen, S. B. Improving dynamic collision frequencies: Impacts on dynamic structure factors and stopping powers in warm dense matter. Physics of Plasmas **2023**, 30, 062703.
- (82) Takada, Y. Emergence of an excitonic collective mode in the dilute electron gas. Phys. Rev. B **2016**, 94, 245106.
- (83) Dornheim, T.; Talias, P.; Moldabekov, Z.; Cangi, A.; Vorberger, J. Effective electronic forces and potentials ab initio path integral Monte Carlo simulations. J. Chem. Phys. **2022**, 156, 244113.
- (84) Hamann, P.; Kordts, L.; Filinov, A.; Bonitz, M.; Dornheim, T.; Vorberger, J. Prediction of a roton-type feature in warm dense hydrogen. Phys. Rev. Res. **2023**, 5, 033039.
- (85) Kadanoff, L. P.; Martin, P. C. Hydrodynamic equations and correlation functions. Annals of Physics **1963**, 24, 419–469.
- (86) Zwanzig, R. Time correlation functions and transport coefficients in statistical mechanics. Annu. Rev. Phys. Chem. **1965**, 16, 67–102.
- (87) Vignale, G.; Ullrich, C. A.; Conti, S. Time-dependent density functional theory beyond the adiabatic local density approximation. Phys. Rev. Lett. **1997**, 79, 4878.
- (88) Conti, S.; Vignale, G. Elasticity of an electron liquid. Phys. Rev. B **1999**, 60, 7966.
- (89) Singwi, K. S.; Tosi, M. P. Correlations in electron liquids. Solid State Physics **1981**, 36, 177–266.
- (90) Böhme, M.; Moldabekov, Z. A.; Vorberger, J.; Dornheim, T. Static Electronic Density Response of Warm Dense Hydrogen: Ab Initio Path Integral Monte Carlo Simulations. Phys. Rev. Lett. **2022**, 129, 066402.

- (91) Böhme, M.; Moldabekov, Z. A.; Vorberger, J.; Dornheim, T. Ab initio path integral Monte Carlo simulations of hydrogen snapshots at warm dense matter conditions. Phys. Rev. E **2023**, 107, 015206.
- (92) Militzer, B.; Ceperley, D. M. Path integral Monte Carlo simulation of the low-density hydrogen plasma. Phys. Rev. E **2001**, 63, 066404.
- (93) Moldabekov, Z.; Schwalbe, S.; Böhme, M.; Vorberger, J.; Shao, X.; Pavanello, M.; Graziani, F.; Dornheim, T. Bound state breaking and the importance of thermal exchange-correlation effects in warm dense hydrogen. 2023.
- (94) Filinov, A. V.; Bonitz, M. The equation of state of partially ionized hydrogen and deuterium plasma revisited. 2023.
- (95) Döppner, T.; Bethkenhagen, M.; Kraus, D.; Neumayer, P.; Chapman, D. A.; Bachmann, B.; Baggott, R. A.; Böhme, M. P.; Divol, L.; Falcone, R. W.; Fletcher, L. B.; Landen, O. L.; MacDonald, M. J.; Saunders, A. M.; Schörner, M.; Sterne, P. A.; Vorberger, J.; Witte, B. B. L.; Yi, A.; Redmer, R.; Glenzer, S. H.; Gericke, D. O. Observing the onset of pressure-driven K-shell delocalization. Nature **2023**, 618, 270.
- (96) Dornheim, T.; Böhme, M.; Kraus, D.; Döppner, T.; Preston, T. R.; Moldabekov, Z. A.; Vorberger, J. Accurate temperature diagnostics for matter under extreme conditions. Nature Communications **2022**, 13, 7911.
- (97) Böhme, M. P.; Fletcher, L. B.; Döppner, T.; Kraus, D.; Baczewski, A. D.; Preston, T. R.; MacDonald, M. J.; Graziani, F. R.; Moldabekov, Z. A.; Vorberger, J.; Dornheim, T. Evidence of free-bound transitions in warm dense matter and their impact on equation-of-state measurements. **2023**,
- (98) Tanaka, S.; Ichimaru, S. Thermodynamics and Correlational Properties of Finite-Temperature Electron Liquids in the Singwi-Tosi-Land-Sjölander Approximation. J. Phys. Soc. Jpn **1986**, 55, 2278–2289.

- (99) Sjostrom, T.; Dufty, J. Uniform Electron Gas at Finite Temperatures. Phys. Rev. B **2013**, 88, 115123.
- (100) Tanaka, S. Correlational and thermodynamic properties of finite-temperature electron liquids in the hypernetted-chain approximation. J. Chem. Phys **2016**, 145, 214104.
- (101) Tanaka, S. Improved equation of state for finite-temperature spin-polarized electron liquids on the basis of Singwi–Tosi–Land–Sjölander approximation. Contributions to Plasma Physics **2017**, 57, 126–136.
- (102) Talias, P.; Lucco Castello, F.; Dornheim, T. Integral equation theory based dielectric scheme for strongly coupled electron liquids. The Journal of Chemical Physics **2021**, 155, 134115.
- (103) Castello, F. L.; Talias, P.; Dornheim, T. Classical bridge functions in classical and quantum plasma liquids. Europhysics Letters **2022**, 138, 44003.
- (104) Talias, P.; Lucco Castello, F.; Dornheim, T. Quantum version of the integral equation theory-based dielectric scheme for strongly coupled electron liquids. The Journal of Chemical Physics **2023**, 158, 141102.
- (105) Dornheim, T.; Vorberger, J.; Moldabekov, Z. A.; Talias, P. Spin-resolved density response of the warm dense electron gas. Phys. Rev. Research **2022**, 4, 033018.
- (106) Dornheim, T. Path-integral Monte Carlo simulations of quantum dipole systems in traps: Superfluidity, quantum statistics, and structural properties. Phys. Rev. A **2020**, 102, 023307.
- (107) Ferré, G.; Boronat, J. Dynamic structure factor of liquid ^4He across the normal-superfluid transition. Phys. Rev. B **2016**, 93, 104510.
- (108) Xiong, Y.; Xiong, H. Thermodynamics of fermions at any temperature based on parametrized partition function. Phys. Rev. E **2023**, 107, 055308.

- (109) Egger, R.; Häusler, W.; Mak, C. H.; Grabert, H. Crossover from Fermi Liquid to Wigner Molecule Behavior in Quantum Dots. Phys. Rev. Lett. **1999**, 82, 3320–3323.
- (110) Paananen, T.; Egger, R.; Siedentop, H. Signatures of Wigner molecule formation in interacting Dirac fermion quantum dots. Phys. Rev. B **2011**, 83, 085409.
- (111) Yan, Y.; Blume, D. Abnormal Superfluid Fraction of Harmonically Trapped Few-Fermion Systems. Phys. Rev. Lett. **2014**, 112, 235301.
- (112) Ceperley, D. M. Fermion nodes. Journal of Statistical Physics **1991**, 63, 1237–1267.
- (113) Militzer, B.; Driver, K. P. Development of Path Integral Monte Carlo Simulations with Localized Nodal Surfaces for Second-Row Elements. Phys. Rev. Lett. **2015**, 115, 176403.
- (114) Müller, F.; Christiansen, H.; Schnabel, S.; Janke, W. Fast, Hierarchical, and Adaptive Algorithm for Metropolis Monte Carlo Simulations of Long-Range Interacting Systems. Phys. Rev. X **2023**, 13, 031006.
- (115) John, C.; Spura, T.; Habershon, S.; Kühne, T. D. Quantum ring-polymer contraction method: Including nuclear quantum effects at no additional computational cost in comparison to ab initio molecular dynamics. Phys. Rev. E **2016**, 93, 043305.